Vol 16 No 9, September 2007
1009-1963/2007/16(09)/2764-05

Chinese Physics

© 2007 Chin. Phys. Soc.
and IOP Publishing Ltd

Formation mechanism of Ge nanocrystals embedded in SiO_2 studied by fluorescence x-ray absorption fine structure*

Yan Wen-Sheng(闫文盛)†, Li Zhong-Rui(李忠瑞),
Sun Zhi-Hu(孙治湖), Pan Zhi-Yun(潘志云), and Wei Shi-Qiang(韦世强)

National Synchrotron Radiation Laboratory, University of Science & Technology of China, Hefei 230026, *China*

(Received 14 July 2006; revised manuscript received 2 February 2007)

This paper reports that the Ge nanocrystals embedded in SiO_2 matrix are grown on Si(100) and quartz–glass substrates, and the formation mechanism is systematically studied by using fluorescence x-ray absorption fine structure (XAFS). It is found that the formation of Ge nanocrystals strongly depends on the properties of substrate materials. In the as-prepared samples with Ge molar content of 60%, Ge atoms exist in amorphous Ge (about 36%) and GeO_2 (about 24%) phases. At the annealing temperature of 1073 K, on the quartz–glass substrate Ge nanocrystals are generated from crystallization of amorphous Ge, rather than from the direct decomposition of GeO_2 in the as-deposited sample. However, on the Si(100) substrate, the Ge nanocrystals are generated partly from crystallization of amorphous Ge, and partly from GeO_2 phases through the permutation reaction with Si substrate. Quantitative analysis reveals that about 10% of GeO_2 in the as-prepared sample are permuted with Si wafer to form Ge nanocrystals.

Keywords: XAFS, local structures, Ge nanocrystals
PACC: 6110, 6155, 8120

1. Introduction

Ge semiconducting nanocrystals embedded in SiO_2 matrix have attracted increasing attention since 1990's due to their unique luminescence properties as well as wide potential applications in optoelectronic and nonvolatile memory devices.[1−6] Magnetron sputtering co-deposition method is commonly used to fabricate Ge nanocrystals embedded in SiO_2 medium, and the effects of preparation conditions on the structure and properties of Ge nanocrystals have been extensively studied.[7−10] Maeda[7] and Fujii *et al*[11] found that the morphology and size of Ge nanocrystals can be strongly affected by Ge content and annealing temperature. However, up to date the formation mechanism of the Ge nanocrystals is still not clear enough. By combining experimental observations and theoretical calculation, Maeda suggested that the precipitation and growth of Ge nanocrystals are related to a thermal reduction of GeO_2, the diffusion of Si atoms from the silicon substrate into glassy matrix, and aggregation of Ge nanocrystal.[7] He also pointed out that the fabrication of Ge nanocrystals by direct decomposition of GeO_2 is thermodynamically impossible under the conventional conditions (around 1.013×10^5 Pa and 1000 K). However, some people believe that Ge nanocrystals are formed through the dissociation of GeO_2 and suboxides in the initial sample.[8,9]

In order to further understand the Ge nanocrystal formation mechanism with and without the involvement of elemental Si atoms, in this work we fabricated Ge nanocrystals embedded in SiO_2 medium with magnetron sputtering method by using two different types of substrate, Si(100) wafer and quartz glass. The local structure changes at Ge sites upon annealing are investigated by x-ray absorption fine structure (XAFS). The XAFS technique has been recognized as a powerful tool for determining the local structure of amorphous materials because of its sensitivity to the short-range order and atomic species surrounding the absorbing atom. Furthermore, one can quantitatively obtain the structural parameters of one element in a complex material by XAFS.[12,13] The deep insight of the Ge nanocrystal formation process has been illustrated by systematically studying the effects of two

*Project supported by the National Natural Science Foundation of China (Grant Nos 10605024, 10375059 and 10404023) and Youth Foundation of University of Science and Technology of China (Grant No KA2310000002).
†Corresponding author. E-mail: ywsh2000@ustc.edu.cn

substrates (Si and SiO_2) on the formation mechanism of Ge nanocrystals.

2. Experimental details

The samples were prepared by co-deposition of Ge and SiO_2 by radio-frequency (RF) magnetron sputtering onto either quartz–glass or Si(100) substrates, under vacuum better than 5×10^{-5} Pa obtained with a cryovacuum pump. The substrate holder was kept at about 300 K by circulating water. A Ge chip ($5 \times 5 \times 1$ mm) of 99.9999% purity was employed as sputtering target. The RF power of 1.5 kW was applied between the target and substrate holder, and the argon partial pressure was held at 0.4 Pa during deposition by using a mass-flow controller. After the deposition, the samples were annealed for 1 h at 800 °C in an argon atmosphere which produced nanocrystals. Both samples have a thickness of about 500 nm and the Ge concentration of 60 mol%. Hereafter, Ge(60%)–SiO_2/Si(100) and Ge(60%)–SiO_2/quartz represent the samples with 60 mol% Ge in the SiO_2 matrix on a Si (100) and quartz substrates respectively. The sizes of the Ge nanocrystals are 20 nm and 5 nm in size for the annealed Ge(60%)–SiO_2/Si(100) and Ge(60%)–SiO_2/quartz respectively, as revealed by the high-resolution transmission electron microscope (HRTEM) images published elsewhere.[14] The Ge K-edge XAFS spectra were collected in fluorescence yield mode at room temperature on beamline BL13B at Photon Factory (2.5 GeV with maximum current of $I_{max} = 400$ mA, Japan) and Beamline 1W1B at Beijing Synchrotron Radiation Facility (2.2 GeV with $I_{max} = 100$ mA, China). XAFS data analysis was performed with UWXAFS 3.0 and NSRLXAFS 3.0 suites.[15,16]

3. Results and discussions

The Ge K-edge x-ray absorption near edge structure (XANES) spectra are displayed in Fig.1 for the as-deposited and the annealed Ge(60%)–SiO_2/Si(100) and Ge(60%)–SiO_2/quartz samples. These two as-deposited samples demonstrate identical XANES features, which suggest that the local structures around Ge are not affected by the properties of the substrates. However, after annealing treatment the Ge K-edge position for Ge(60%)–SiO_2/Si(100) is shifted to lower energy by 1.4 eV, while that for Ge(60%)–SiO_2/quartz sample keeps unchanged upon annealing. Since the Ge K-edge XANES arises from the transition of Ge 1s electron to unoccupied 4 p states, the downward shift of the Ge absorption edge means that the Ge 4p states are moved to lower energy side. This is mainly due to the reduced valence of Ge, which decreases the orbital overlapping between Ge atom and the ligands around it, and weakens the repulsive force between them. Hence, we can see that annealing can reduce the average covalence of Ge in the Ge(60%)–SiO_2/Si(100), but has no effect on the valence of Ge in Ge(60%)–SiO_2/quartz sample. The Ge atoms in these two samples have different thermodynamical behaviours during the annealing treatment.

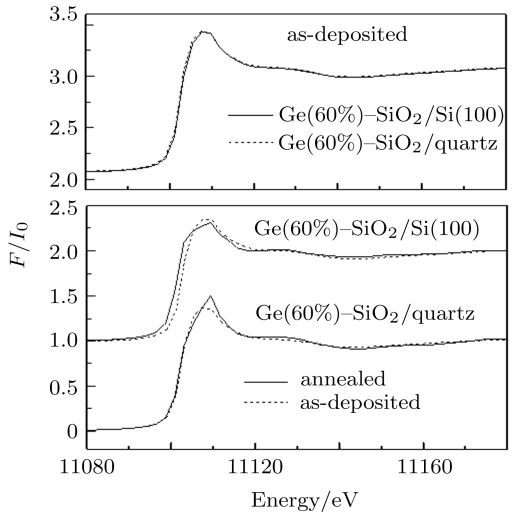


Fig.1. Ge K-edge XANES of Ge(60%)–SiO_2/Si(100) and Ge(60%)–SiO_2/quartz before and after annealing.

Figure 2(a) shows the Ge K-edge EXAFS functions ($\chi(k)$) of the as-deposited and the annealed Ge(60%)–SiO_2/Si(100) and Ge(60%)–SiO_2/quartz samples. It is evident that the oscillation frequencies of the $\chi(k)$ functions for Ge(60%)–SiO_2/Si(100) and Ge(60%)–SiO_2/quartz samples keep almost unchanged upon annealing, while the oscillation amplitudes exhibit an opposite tendency. In the low k-region ($k < 6$ Å^{-1}), the oscillation amplitude of the Ge(60%)–SiO_2/quartz sample increases remarkably, while that of the Ge(60%)–SiO_2/Si(100) sample decreases considerably. It indicates that the Ge local structure on the two different substrates changes differently after annealing. To more clearly illustrate the local structure change on the two different substrates caused by the annealing treatment, Fig.2(b) shows the radial structure functions (RSFs) of Ge obtained by Fourier transforming the k^2-weighted EXAFS functions. The RSFs of the as-deposited Ge(60%)–

SiO_2/quartz and Ge(60%)–SiO_2/Si(100) present remarkable difference from those of crystal Ge and GeO_2. The coordination peaks at 1.4 and 2.1 Å correspond to the first shells of bulk GeO_2 (Ge–O) and Ge (Ge–Ge) respectively, but no peaks at 2.8 and 3.5 Å corresponding to the higher coordination shells of GeO_2 and Ge can be observed. Therefore, in the as-deposited samples, part of Ge atoms exists in the form of pure Ge phase, and another part in the form of GeO_2. This is consistent with the XPS result of Maeda *et al.*[7,17] On the other hand, the as-deposited Ge(60%)–SiO_2/quartz and Ge(60%)–SiO_2/Si(100) samples also exhibit amorphous character as revealed by the x-ray diffraction (XRD) result of Frenkel *et al*[18] and our previous Raman spectra.[14] All these results lead us to conclude that the Ge atoms in the as-deposited samples exist in the form of amorphous Ge and amorphous GeO_2. Interestingly, after the annealing treatment at 1073 K, the Ge–O coordination peaks of Ge(60%)–SiO_2/Si(100) and Ge(60%)–SiO_2/quartz changed differently. The RSF intensity of Ge–O coordination shell decreased by 30% for Ge(60%)–SiO_2/Si(100), while that of Ge(60%)–SiO_2/quartz increased by about 30%. Additionally, at long distance the two annealed samples display similar Ge-Ge coordination peaks as bulk Ge. It is obvious that the silicon or quartz substrate plays distinct role in the formation of Ge nanocrystals.

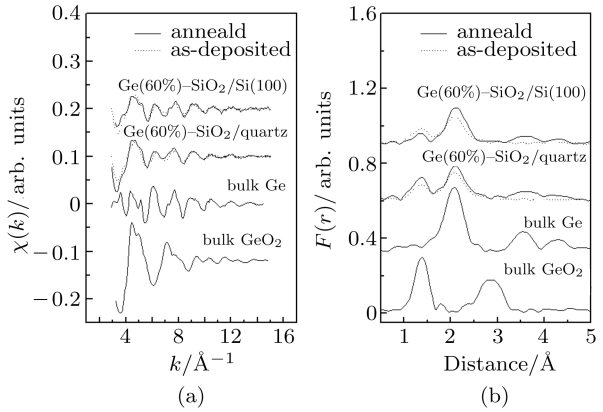


Fig.2. (a) The Ge K-edge EXAFS oscillations, (b) the RSFs of Ge(60%)–SiO_2/Si(100) and Ge(60%)–SiO_2/quartz before and after annealing. Those of bulk Ge and GeO_2 are also included for comparison.

For quantitative analysis, the least-squares curve fit was performed by using the USTCXAFS3.0 code,[16] and the theoretical amplitude functions calculated by FEFF8.[19] Since the annealing temperature used in this work is much lower than the temperature at which Ge–Si alloying can occur (above 1173 K), we can neglect the Ge–Si bond in the fitting. The filtered data using the R-range including both Ge–Ge and Ge–O pairs (1.0 to 2.7 Å range), together with the result of the least-squares curve fitting based on a single scattering theory are shown in Fig.3 to demonstrate the quality of the fit. The good fitting quality provides additional evidence that Ge–Si bonds are not presented in our samples. The structural parameters obtained for all samples are summarized in Table 1.

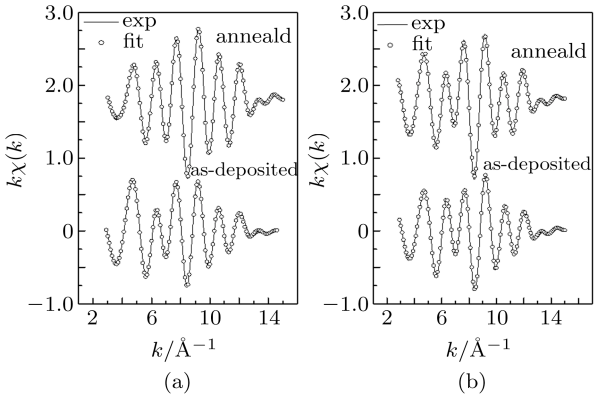


Fig.3. The curve-fitting results for samples before and after annealing: (a) Ge(60%)–SiO_2/Si(100), and (b) Ge(60%)–SiO_2/quartz.

Table 1. The local structural parameters of Ge sites for Ge(60%)–SiO_2/Si(100) and Ge(60%)–SiO_2/quartz before and after annealing treatment.

Sample	Bond type	R/Å	σ/Å	N	%*
Ge(60%)–SiO_2/Si(100) as-deposited	Ge–O	1.74±0.01	0.064±0.003	1.5±0.3	24%
	Ge–Ge	2.45±0.01	0.073±0.003	2.5±0.4	36%
Ge(60%)–SiO_2/Si(100) annealed	Ge–O	1.73±0.01	0.061±0.003	1.0±0.3	15%
	Ge–Ge	2.45±0.01	0.064±0.003	3.2±0.3	45%
Ge(60%)–SiO_2/quartz as-deposited	Ge–O	1.75±0.01	0.064±0.003	1.3±0.3	24%
	Ge–Ge	2.45±0.01	0.072±0.003	2.4±0.4	36%
Ge(60%)–SiO_2/quartz annealed	Ge–O	1.73±0.01	0.055±0.003	1.4±0.3	24%
	Ge–Ge	2.45±0.01	0.061±0.003	2.5±0.4	36%

*The value on the Ge–O line refers to the GeO_2 concentration, while in Ge–Ge line it refers to the concentration of Ge clusters in the sample.

As shown in Table 1, the first shell Ge–O coordination number of GeO_2 species in Ge(60%)–SiO_2/Si(100) decreases from 1.5 to 1.0 after annealing treatment, and at the same time the Ge–Ge coordination number increases from 2.5 to 3.2. But for the Ge(60%)–SiO_2/quartz sample the coordination numbers of Ge–O and Ge–Ge shells did not change much. Based upon these coordination numbers and Lu's EXAFS analysis approach for mixed phase,[20] we estimated the concentration of Ge and GeO_2 species in the samples (see Table 1). It can be found that the concentration of GeO_2 species in the annealed Ge(60%)–SiO_2/quartz did not change basically, but that of Ge(60%)–SiO_2/Si(100) decreased by 10%. This indicates that in Ge(60%)–SiO_2/Si(100), part of GeO_2 was converted into Ge nanocrystal while no GeO_2 in the Ge(60%)–SiO_2/quartz participated in the formation of nanocrystal Ge.

There are two possible paths for the conversion of GeO_2 into Ge nanocrystal in our samples: one is the decomposition of GeO_2, which was thermodynamically unfavorable under our annealing conditions as pointed out by Maeda;[7] another is the silicon-involved reduction, i.e. $GeO_2+Si \rightarrow Ge+SiO_2$. On the quartz substrate no elemental Si atoms exist, so the reduction reaction cannot occur. Additionally, the concentrations of GeO_2 and Ge phases are not affected by the annealing treatment in the Ge(60%)–SiO_2/quartz sample. All these results illustrate that the GeO_2 embedded in SiO_2 cannot decompose by itself to form Ge nanocrystals, and the Ge nanocrystals can only originate from the amorphous Ge in the as-deposited Ge(60%)–SiO_2/quartz. But, on the Si substrate, GeO_2 might be another important source for the formation of Ge nanocrystal. The electron microscopic analysis made by Maeda has revealed that the Si atoms can diffuse from the Si(100) substrate into SiO_2 layer.[7] The elemental Ge is thermodynamically very stable in a SiO_2 matrix, and this displacement reaction ($GeO_2+Si \rightarrow Ge+SiO_2$) can proceed spontaneously at the interface between GeO_2 and Si under the annealing temperature. Hence, for the Ge(60%)–SiO_2/Si(100) sample, part of the Ge nanocystals are generated from GeO_2 through the permutation reaction with the silicon atoms diffused from the Si(100) substrate.

Our previous electron microscopy analysis[14] has revealed that the Ge nanocrystals formed on quartz substrate have a uniform size of about 5 nm, while those on Si(100) wafer have a mean size of 20 nm with a wide distribution. On quartz substrate Ge nanocrystals are directly converted from amorphous Ge phase and their sizes are quite uniform. On the contrary, on the silicon wafer, besides part of Ge nanocrystals from amorphous Ge phase, part of GeO_2 species are reduced into atomic Ge through the reaction with Si atoms ($GeO_2+Si \rightarrow Ge+SiO_2$). These reduced Ge atoms can aggregate with the Ge nano-crystals formed from the amorphous Ge, and as a consequence, the Ge nanocrystals produced on silicon wafer have a larger average size and a wider distribution. It means that under the same annealing conditions, on quartz substrate we can produce even sized Ge nanocrystal with prominent quantum size effect.[21] Maeda observed that the properties of photoluminescence in the visible range show a strong correlation to the change in size.[7] Hence, a blue-shift of photoluminescence is expected when we switch the substrate from Si wafer to quartz.

4. Conclusions

Ge nanocrystals embedded in SiO_2 matrix can be fabricated on either Si or quartz substrate by magnetron sputtering and subsequent annealing treatment. Ge nanocrystals in Ge(60%)–SiO_2/quartz are generated from amorphous Ge clusters in the as-deposited sample, but not from the direct decomposition of GeO_2. As to Ge nanocrystal particles in Ge(60%)–SiO_2/Si(100), besides part of them originating from amorphous Ge particles, part of them are generated by the permutation reaction between GeO_2 and the silicon atoms diffused from the Si(100) substrate. Additionally, Ge nanocrystal originated from the permutation reaction is expected to have larger size in comparison with that from amorphous Ge under the annealing temperature of 1073 K. So by switching the substrate from Si wafer to quartz, we can achieve smaller sized and uniform Ge nanocrystals, which lead to a blue-shift in photoluminescence band.

Acknowledgments

We are grateful to KEK and BSRF for giving us the XAFS beam time.

References

[1] Takagi H, Ogawa H, Yamazaki Y, Ishizaki A and Nakagiri T 1990 *Appl. Phys. Lett.* **56** 2379

[2] Banerjee S, Nozaki S and Morisaki H 2000 *Appl. Phys Lett.* **76** 445.

[3] Duguay S, Grob J J, Slaoui A, Le Gall Y and Amann-Liess M 2005 *J. Appl. Phys.* **97** 104330

[4] Wang Y Y, Yang Y H, Guo Y P, Gan R J, He Y, Xue H and Chen G H 1997 *Acta Phys. Sin.* **46** 203 (in Chinese)

[5] He Z H, Chen K J and Feng D 1997 *Acta Phys. Sin.* **46** 1153 (in Chinese)

[6] Liu S R, Huang W Q and Qin C J 2006 *Acta Phys. Sin.* **55** 2488 (in Chinese)

[7] Maeda Y 1995 *Phys. Rev.* B **51** 1658

[8] Choi W K, Ho Y W, Ng S P and Ng V 2001 *J. Appl. Phys.* **89** 2168

[9] Jiang N, Qiu J R and Spence J C H 2005 *Appl. Phys. Lett.* **86** 143112

[10] Wa S Y, Qin G G, You P and Wang Y Y 2001 *Acta Phys. Sin.* **50** 1580 (in Chinese)

[11] Fujii M, Hayashi S and Yamamoto K 1990 *Appl. Phys. Lett.* **57** 2692

[12] Liu T, Hu T D, Xie Y N, Jiang H Y, Wang D W, Wang W D and Li H B 1998 *Chin. Phys.* **7** 541

[13] Yan W S, Yin S L, Fan J W, Li Y Z, Liu W H, Hao L Y, Pan Z Y and Wei S Q 2005 *Acta Phys. Sin.* **54** 5707 (in Chinese)

[14] Kolobov A V, Wei S Q, Yan W S, Maeda Y and Tanaka K 2003 *Phys. Rev.* B **67** 195314

[15] Newville M, Līviņš P, Yacoby Y, Rehr J J and Stern E A 1993 *Phys. Rev. B* **47** 14126

[16] Zhong W J and Wei S Q 2001 *Journal of University of Science and Technology of China* **31** 328

[17] Maeda Y, Tsukamoto N, Yazawa Y, Kanemitsu Y and Masumoto Y 1991 *Appl. Phys. Lett.* **59** 3168

[18] Frenkel A I, Kolobov A V, Robinson I K, Cross J O, Maeda Y and Bouldin C E 2002 *Phys. Rev. Lett.* **89** 285503

[19] Ankudinov A, Ravel B, Rehr J J and Conradson S D 1998 *Phys. Rev.* B **58** 7565

[20] Lu K Q and Wan J 1987 *Phys. Rev.* B **35** 4497

[21] Takeoka S, Fujii M, Hayashi S and Yamamoto K 1998 *Phys. Rev.* B **58** 7921